JOURNAL OF MAGNETIC RESONANCE **128,** 207–216 (1997)
ARTICLE NO. MN971221

Origin of the Correlation Time Dependence of Coherence Transfer Distortions in Rotating Frame Cross-Relaxation Spectra

Ranajeet Ghose,* C. Anderson Evans,† and James H. Prestegard*,[1]

*Department of Chemistry, Yale University, New Haven Connecticut 06520; and †Schering-Plough Research Institute, Kenilworth, New Jersey 07033

Received March 11, 1997; revised July 7, 1997

HOHAHA distortions in conventional (CW) ROESY experiments are known to be prominent when the frequency of the spin-lock field is near the midpoint between the resonance frequencies of a pair of coupled spins. That the disappearance of these distortions with offset from the midpoint is more rapid for large molecules than smaller ones is less widely known, and less well understood. We provide a quantitative explanation of the latter phenomenon using a combination of theory and numerical simulations. The cause of this effect can be found in the differential relaxation of the various magnetization modes which are involved in HOHAHA transfer. These modes experience enhanced relaxation far from a Hartmann–Hahn match. This enhancement is larger for molecules which have long correlation times.

Key Words: **ROESY; HOHAHA; correlation time; magnetization modes; average relaxation time.**

INTRODUCTION

A long standing problem in the quantitative interpretation of rotating frame Overhauser, i.e., CAMELSPIN (*1*) and ROESY (*2*), experiments in scalar coupled spin systems is that the peaks induced by cross-relaxation are distorted due to antiphase COSY-type and inphase HOHAHA-type (*3*) transfers. The distortions of the latter kind are more significant since the COSY-type distortions have no significant effect on the crosspeak volume integral. Several pulse sequence modifications have been proposed to obtain ROESY spectra with minimum HOHAHA distortions (*4–6*). It is important to note that there exists a theoretical minimum amount of HOHAHA distortion which must be accepted in ROESY spectra (*6*). HOHAHA transfers may also be reduced in conventional ROESY spectra by a careful choice of the spin-lock transmitter offset (*7*). Chan *et al.* (*7*) recently proposed a simple procedure based on a COSY spectrum to make this choice. Crosspeaks between coupled resonances in a COSY spectrum lie on a line perpendicular to the diagonal at a transmitter position which is exactly halfway between the resonances. This line also corresponds to the condition of maximum HOHAHA transfer. Thus, choosing a transmitter position where there are no crosspeaks perpendicular to the diagonal minimizes HOHAHA distortions in conventional ROESY spectra. In this same publication Chan *et al.* report the observation of a molecular weight dependence of the range of transmitter positions over which the HOHAHA distortions occur. The effects drop off more rapidly for large molecules than for small molecules. This dependency is of some practical utility, since avoiding the HOHAHA distortions becomes easier for larger molecules. Only a qualitative explanation for this molecular weight dependence could be given at that time. Here we make that explanation more quantitative using a combination of theory and numerical results utilizing the magnetic resonance simulation library GAMMA (*8*).

THEORY

For the pulse sequence shown in Fig. 1, the portion of the density matrix capable of generating a $k \rightarrow l$ crosspeak in a simple two-spin (k, l) system is given by I_{ky} at the beginning of the t_1 period with evolution during the t_1 period generating additional terms such as I_{kx}, $2I_{ky}I_{lz}$, and $2I_{kx}I_{lz}$. It should be realized that terms evolving as antiphase during the t_1 period ($2I_{ky}I_{lz}$, $2I_{kx}I_{lz}$) have vanishing integrals and hence do not contribute to the crosspeak volume. Also, under relatively strong spin-lock conditions, with the spin-lock field along the y axis, only those parts of the density matrix which are proportional to I_{ly} at the beginning of the detection period (i.e., $t_2 = 0$) contribute to the volume of the $k \rightarrow l$ crosspeak. The measured volume of the $k \rightarrow l$ crosspeak is, thus, proportional to the sum of the expectation value of I_{ly} evaluated using a density matrix σ which evolved from either I_{kx} or I_{ky} at the start of the spin-lock period. Mathematically, the $k \rightarrow l$ crosspeak volume can be represented by

$$(\text{volume})_{k\rightarrow l} = K_1\left[\frac{\text{Tr}[I_{ly}\sigma(\tau)]}{\text{Tr}[I_{ly}^{*}I_{ly}]}\bigg|_{\sigma(\tau=0)=I_{kx}}\right] + K_2\left[\frac{\text{Tr}[I_{ly}\sigma(\tau)]}{\text{Tr}[I_{ly}^{*}I_{ly}]}\bigg|_{\sigma(\tau=0)=I_{ky}}\right], \quad [1]$$

[1] To whom all correspondence should be addressed. E-mail: james.prestegard@yale.edu.

1090-7807/97 $25.00

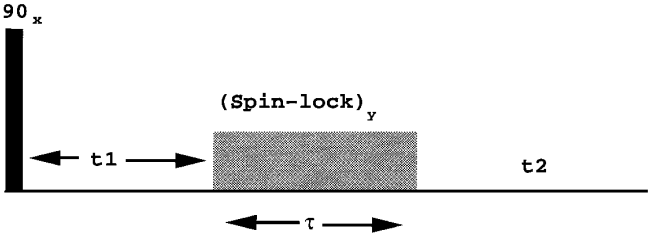

FIG. 1. Basic pulse-sequence used in the experiment of (*6*) and also in the full 2D simulations.

where K_1 and K_2 are constants of proportionality which depend on the evolution during t_1. In the most general case, for long enough evolution times, I_{kx} and I_{ky} are sampled equally, in which case $K_1 = K_2$. On Fourier transformation in t_1, the same holds true, since the functional dependence of K_1 and K_2 on t_1 is transferred to the lineshape in the indirect dimension.

During the spin-lock period, terms such as $2I_{ky}I_{lz}$ and $2I_{kx}I_{lz}$ are generated from I_{kx} and I_{ky}. As is shown in the Appendix, most of these terms do not commute with the spin-lock Hamiltonian and hence precess during the spin-lock period. In most probes the applied RF field of the spin lock is inhomogeneous in both phase and magnitude, i.e., the spin-lock field varies as function of position in the sample. The magnitude variation causes most of the density matrix components from the above terms to have different oscillation frequencies at different positions in the sample, and this alone will result in the net signal from most of these components averaging to zero over the sample volume at sufficiently long spin-lock times (*9*). However, those parts of the $2I_{kx}I_{lz}$ term which transform to zero-quantum coherence in the spin-lock frame behave differently. These zero-quantum components (in the frame of the spin lock) precess very slowly for homonuclear systems and are therefore far less sensitive to field inhomogeneity. They, along with I_{ly} persist at the end of the spin-lock period and are primarily responsible for crosspeak intensity in the strong field limit.

It is to be mentioned here that for sufficiently strong spin-lock fields, when both spins are locked near resonance (with the spin-lock field along the *y* axis) there is no appreciable interconversion between I_{kx} and I_{ky} during the course of the spin lock. The interconversion between I_{kx} and $2I_{ky}I_{lz}$ still occurs, but since both these terms are significantly affected by the inhomogeneity, their effects on the expectation value of I_{ly} average out over the sample volume. Under those conditions the first term of [1] may be neglected. However, when spin-lock fields of moderate strength are used, it is not possible to lock both spins on or near resonance. Even when the density operator at the beginning of the spin-lock period is I_{kx}, evolution during the spin-lock period generates terms such as I_{ky} which are far more efficient than I_{kx} itself in creating I_{ly}. Under these moderate spin-lock conditions, it is not possible to neglect the first term of [1]. This is because even though the net signal from I_{kx} is attenuated by the field inhomogeneity, some of the terms created from it lead to signal (i.e., I_{ly}). This is the case in our simulations.

The above discussion lays a basis for the proper prediction of the crosspeak intensity as a function of the coupling between the spins, RF field strength, and precession frequencies of the spins in question. It does not, however, address the difference in this functional dependence when molecules of different molecular weights are examined. In order to understand the molecular weight dependence, we need to explicitly consider relaxation effects during the spin-lock period.

Formally, the evolution of the density matrix in the presence of spin relaxation can be obtained by integrating the Liouville–von Neumann equation (*10*)

$$\frac{d\sigma}{dt} = -i\mathcal{H}\sigma + \Gamma[\sigma - \sigma_{\text{eq}}], \qquad [2]$$

where σ_{eq} is the density matrix at thermal equilibrium, and $\mathcal{H}$ and Γ are the Hamiltonian and relaxation superoperators respectively. The solution to [2] is given by

$$\sigma(\text{t}) = e^{\mathcal{L}t}[\sigma(\text{t}) - \sigma_\infty] + \sigma_\infty, \qquad [3]$$

where $\mathcal{L}$ is the Liouville superoperator given by $\mathcal{L} = -i\mathcal{H} + \Gamma$, and σ_∞ is the steady-state density matrix (which is different from σ_{eq} in the presence of the RF field of the spin lock). We have used functions included in the GAMMA (*8*) library to simulate the effects of relaxation during the spin-lock period. The relaxation properties of the spin system were determined using the full Redfield relaxation matrix (*11*) modified to account for the mixing of the various spin states in the presence of the RF field of the spin lock (*12*). The secular approximation was not invoked since the mixing of the spin states caused by the presence of the RF field could cause certain nonsecular terms to contribute significantly to the relaxation. σ_∞ may be formally expressed in terms of σ_{eq} as (*13*)

$$\sigma_\infty = \mathcal{L}^{-1}[\Gamma\sigma_{\text{eq}}]. \qquad [4]$$

However, since $\mathcal{L}$ is singular and so does not possess an inverse, [4] cannot be evaluated directly. The calculation of σ_∞ was performed using the method outlined by Ravikumar *et al.* (*14*) as implemented in the GAMMA routines.

SIMULATIONS AND DISCUSSION

The spins *k* and *l* were taken to be protons with chemical shifts of 1800 and 600 Hz respectively, and the size of the coupling between them was taken to be 7 Hz. The spectrome-

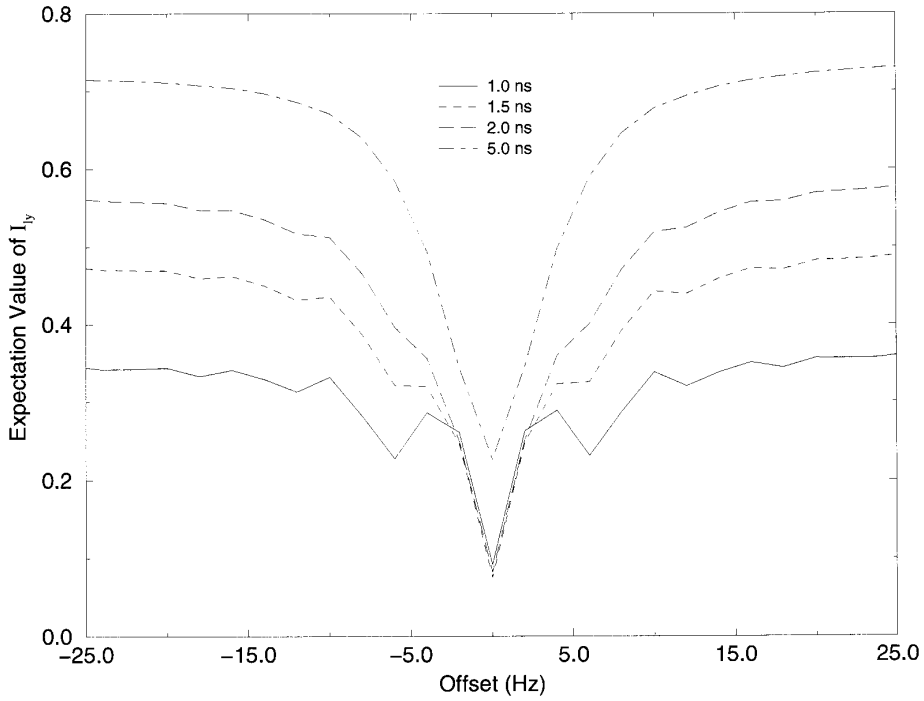

FIG. 2. Plot of the expectation value of I_{ly} against offset from perfect Hartmann–Hahn match when the field at the edges of the sample tube was 20% of its maximum value (at the center of the sample tube) and the initial density operator was I_{ky}.

ter frequency was 400.13 Hz, and the $k - l$ internuclear distance was 2.3 Å. The calculations were performed for positions of the spin-lock carrier from 1150 to 1250 Hz in 2-Hz increments, for correlation times of 0.5, 0.8, 1.0, 1.5, 2.0, 2.5, and 5.0 ns (isotropic Brownian motion assumed). A spin-lock time of 400 ms was used, and the strength of the spin-lock field was taken to be 2300 Hz. In order to include the effects of inhomogeneity, the amplitude of the spin-lock field was taken to be quadratic with respect to position in the sample:

$$\omega_1(r) = \omega_1[1 - kr^2]. \qquad [5]$$

k was chosen such that the field at the edges of a 1-cm sample drops to either 40 or 20% of its maximum value at the center of the sample ($r = 0$). The sample was divided into 1000 volume elements, and the results were averaged over these volume elements. Inhomogeneity in the spin-lock field could in principle originate from variation of the phase of the spin-lock field in addition to its amplitude. Random phase variations also contribute a reduction of the amplitude of the effective field along the spin-lock direction. While there may be some unique contributions due to phase variations, we have, for simplicity, considered only the effects of a somewhat exaggerated amplitude variation in this paper.

Representative results of the simulations are shown in Figs. 2, 3, and 4. Figure 2 deals with the $I_{ky} \rightarrow I_{ly}$ transfer. A detailed product operator analysis of coherence transfer effects in the presence of a spin-lock field has been carried out by Bazzo and Boyd (*15*), we will not reproduce it here. Instead, we will explain the general features of the simulated curves. It is observed that the expectation value of I_{ly} at the end of the spin-lock period is an oscillating function of the spin-lock carrier position. This is especially evident for the shorter correlation times. This arises primarily because transfer to and from I_{ky} during the spin-lock is itself an oscillatory function of τ and the frequency of this oscillation is offset dependent. For sufficiently strong spin-lock fields, it can be shown that the frequency of the temporal oscillations is given by (*16*)

$$\Omega = J\left[1 + \left(\frac{\omega_k^{e^2} - \omega_l^{e^2}}{2J\omega_1}\right)^2\right]^{1/2}, \qquad [6]$$

where ω_k^e and ω_l^e are the effective precession frequencies (in the frame of the spin lock, see Appendix) of the spins k and l respectively. It is evident that this frequency can be very large at large offsets and approaches the coupling constant J as one approaches Hartmann–Hahn match. When we detect I_{ly} after a fixed spin-lock time, these offset dependent temporal oscillations transform into offset oscillations. The oscillations are significantly damped with the introduction of lock field inhomogeneity, especially those oscillations which occur at large offsets. Those which are relatively close

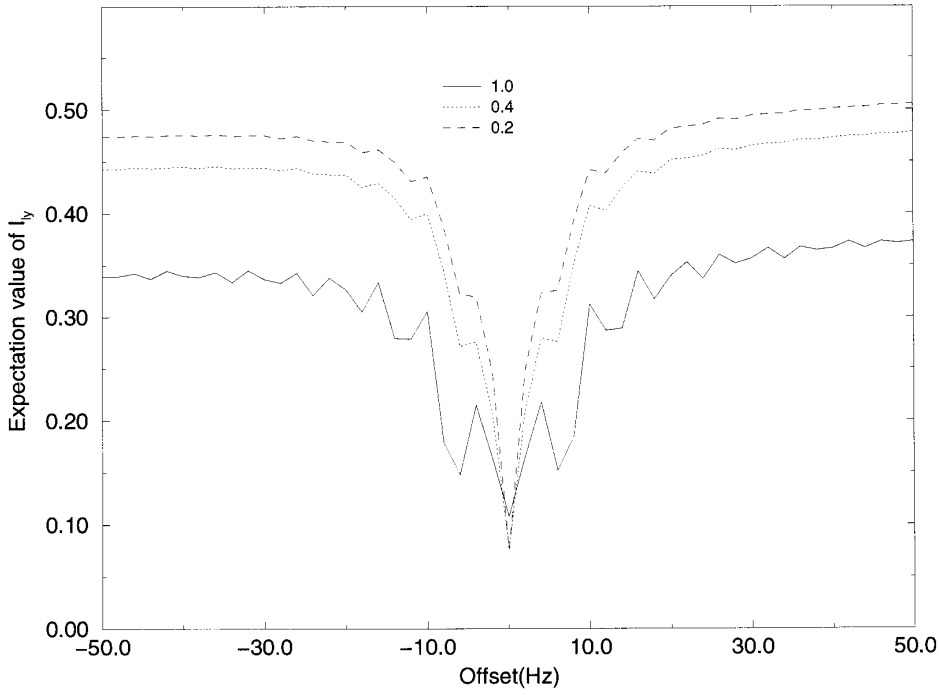

FIG. 3. Plot of the expectation value of I_{ly} against offset from perfect Hartmann–Hahn match when the initial density operator was I_{ky} for various values of the amplitude of the lock field at the edge of the sample as a fraction of the maximum amplitude (at the sample center). Correlation time = 1.5 ns.

to the Hartmann–Hahn match condition (i.e., at an offset of 0) seem to be less susceptible to inhomogeneity effects. They are caused by the creation of $2I_{kx}I_{lz}$ from I_{ky}. Parts of $2I_{kx}I_{lz}$ which transform to zero-quantum terms in the frame of the spin lock are not affected by lock inhomogeneity. These parts persist and are partially converted to I_{ly} at the end of the spin lock. The zero-quantum terms also have a temporal oscillation which is dependent on carrier position, but the dependence is more subtle in this case. The oscillation depends on the lock angles of the two spins and the scalar coupling between them. The amplitude of this oscillation (as a function of offset) increases sharply as one approaches a position where the spin-lock carrier is exactly halfway between the two spins, i.e., where the Hartmann–Hahn match condition is fulfilled.

Superimposed on the above oscillatory (as a function of offset) transfers is the creation of I_{ly} from I_{ky} due to cross-relaxation, i.e., ROESY effects. This does not have an appreciable dependence on the carrier position for sufficiently strong spin-lock fields. These cross-relaxation effects (which tend to raise the baseline of the plots in Figs. 2, 3, and 4) become more pronounced for longer correlation times, and this explains the large expectation values of I_{ly} even at relatively large offsets. These cross-relaxation effects also tend to have a damping effect on the oscillations caused by through-bond HOHAHA effects (*16*). The transfers due to cross-relaxation effects have an opposite sign compared to those due to HOHAHA effects. The net contribution of these two effects to the expectation value of I_{ly} is what is depicted in Fig. 2.

The pronounced oscillations seen in Fig. 2 are rarely observed in experimental data. A possible explanation for this could be the fact that in experimental situations, the spin-lock field is somewhat unstable over the spin-lock time in addition to being inhomogeneous (in phase and amplitude) over the sample volume. The effect of RF field amplitude inhomogeneity on the oscillations in the expectation value of I_{ly} is depicted in Fig. 3. It is also seen from Fig. 3 that there is a change in the expectation values of I_{ly} even at large offsets as the inhomogeneity in the RF field changes. This is because, in the presence of inhomogeneity, spins closer to the edge of the sample experience only a fraction of the spin-lock field; this affects their cross-relaxation properties.

Figure 4 shows the effects of carrier position on the $I_{kx} \rightarrow I_{ly}$ transfer. These curves display a lack of pronounced oscillations (compared to the $I_{ky} \rightarrow I_{ly}$ case). Far from Hartmann–Hahn match, the expectation value is seen to increase with the increase in correlation time due to the fact cross-relaxation effects become more efficient with an increase in the correlation time. Close to Hartmann–Hahn match, there is a mutual transfer of magnetization between I_{ly} and I_{ky} which was created from I_{kx} during the spin-lock period. The lack of oscillations in these curves is due to the fact that

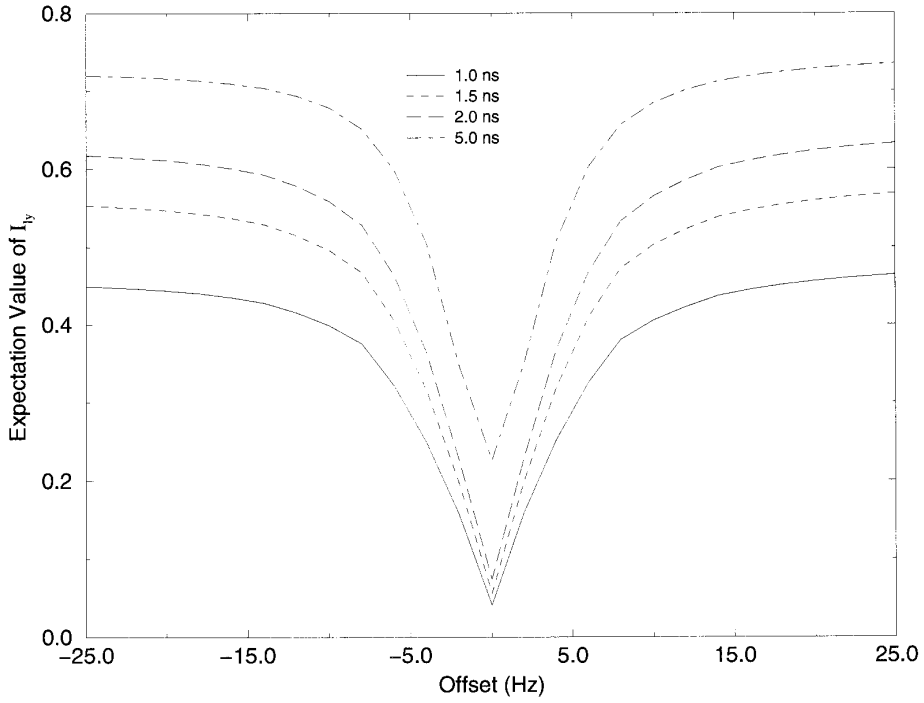

FIG. 4. Plot of the expectation value of I_{ly} against offset from perfect Hartmann–Hahn match when the field at the edges of the sample tube was 20% of its maximum value (at the center of the sample tube) and the initial density operator was I_{kx}.

they are dominated by cross-relaxation. It is evident that effects of the zero-quantum terms do not play a major role in this case since these terms cannot be directly created from I_{kx} (for reasonable spin-lock field strengths).

Having simulated the basic features of the buildup of the expectation values of I_{ly} we now proceed to tackle our original problem, namely the fact that the onset of HOHAHA effects is attenuated more effectively with frequency offset for larger molecules with longer correlation times than for smaller molecules with shorter correlation times. It is possible to see trends toward a sharper offset dependence with an increase in correlation time from the plots with different correlation times in Figs. 2 and 4. However, in order to present this more clearly, it is necessary to sum the expectation values of I_{ly} obtained from the two pathways, shown in Figs. 2 and 4. In summing the contributions from the two pathways we have assumed that $K_1 = K_2$ in [1]. The curves obtained by plotting the sum of the expectation value of I_{ly} obtained from the two paths namely $I_{kx} \rightarrow I_{ly}$ and $I_{ky} \rightarrow I_{ly}$, as a function of offset from Hartmann–Hahn match, were fitted to Lorentzians in order to have an uniform measure of the ''bandwidth at half-height'' of HOHAHA onset. Figure 5 shows a plot of the bandwidth of HOHAHA onset plotted against correlation time for various degrees of RF field inhomogeneity. It can be seen that the effects of inhomogeneity tend to decrease the bandwidth irrespective of the correlation time. This is because several pathways which cause creation of I_{ly}, especially those involving some of the antiphase terms which are susceptible to inhomogeneity effects, tend to become less efficient as the inhomogeneity increases.

In order to provide some insight into the origin of the change in the bandwidth of HOHAHA onset with correlation time in the simulations and discussion above, it is useful to transform into the frame of the spin-lock field (see Appendix) and describe the dynamics of the spin system in terms of specific magnetization modes. In certain limiting situations, these modes have a simple relationship to the regular spin operators we have used in the presentation above. We focus on the magnetization mode responsible for HOHAHA transfer and apply previously derived analytical formulas in those specific limits. Transforming into the doubly tilted frame of the spin lock, this mode is given by $1/2(I_{kz'} - I_{lz'})$ where $I_{kz'}$ and $I_{lz'}$ are the spin operators in the tilted frame (see Appendix); we call this mode M_1. The inversion of this mode (in the absence of relaxation effects) corresponds to a complete transfer of magnetization from $k \rightarrow l$. M_1 is periodically converted into two other modes M_2 and M_3 which are given by $1/2(I_{k+'}I_{l-'} + I_{k-'}I_{l+'})$ and $i/2(I_{k-'}I_{l+'} - I_{k+}I_{l-'})$ respectively. The evolution of M_1, M_2, and M_3 during the spin-lock period τ is given by (*17*)

$$M_1(\tau) = M_1[\cos^2\phi + \sin^2\phi \cos(2q\tau)] + M_2\left[\frac{\sin(2\phi)}{2}(1 - \cos(2q\tau))\right] - M_3[\sin\phi \sin(2q\tau)] \quad [7a]$$

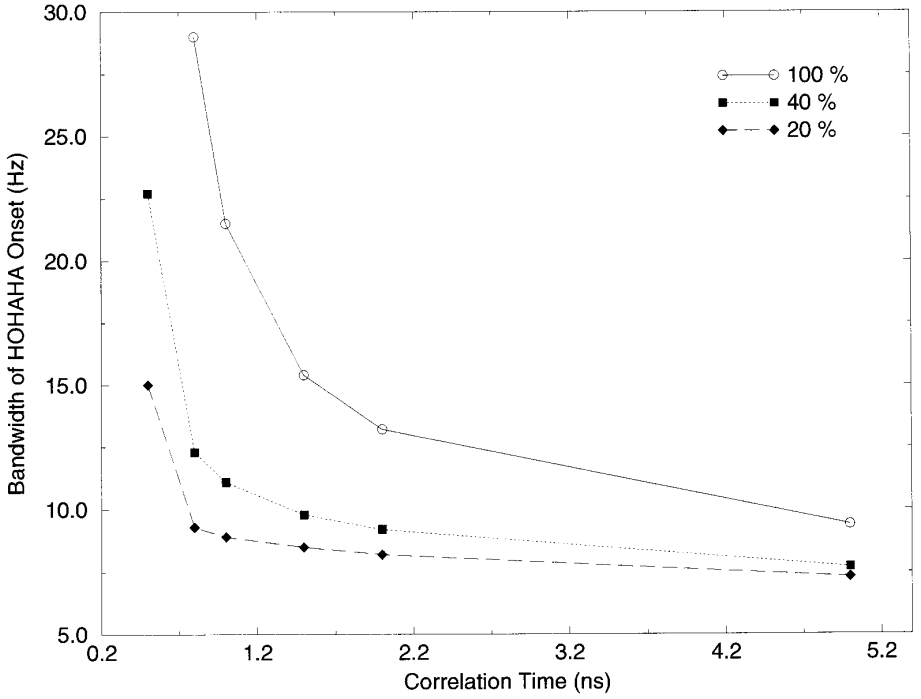

FIG. 5. Plot of the bandwidth of HOHAHA onset against correlation time for the change in the summed expectation values of I_{ly} with change in the position of the spin-lock transmitter for $I_{kx} \rightarrow I_{ly}$ and $I_{ky} \rightarrow I_{ly}$ pathways. The percentages in the figure refer to the field strength at the edges of the sample as a fraction of its maximum value (at the center of the sample).

$$M_2(\tau) = M_1\left[\frac{\sin(2\phi)}{2}(1 - \cos(2q\tau))\right] + M_2[\sin^2\phi + \cos^2\phi\cos(2q\tau)] + M_3[\cos\phi\sin(2q\tau)] \quad [7b]$$

$$M_3(\tau) = M_1[\sin\phi\sin(2q\tau)] - M_2[\cos\phi\sin(2q\tau)] + M_3[\cos(2q\tau)], \quad [7c]$$

where $\phi = \tan^{-1}\{\pi J[\sin(\theta_k)\sin(\theta_l)]/(\omega_k^e - \omega_l^e)\}$ and $q = 1/2\{(\omega_k^e\omega_l^e)^2 + [\pi J\sin(\theta_k)\sin(\theta_l)]^2\}^{1/2}$. The other terms are the same as those defined in the Appendix. In addition to the above three modes, a fourth mode must be considered; this mode, although not converted into the above three modes due to evolution during the spin-lock time, is linked to M_1 by cross-relaxation. This mode, which we call M_4, is given by $1/2(I_{kz'} + I_{lz'})$. The time evolution of the various modes is given by the coupled differential equations

$$\frac{d}{dt}\begin{pmatrix} M_1 \\ M_2 \\ M_3 \\ M_4 \end{pmatrix} = \begin{pmatrix} -R_{11}^{av} & -R_{12}^{av} & -J' - R_{13}^{av} & -R_{14}^{av} \\ -R_{12}^{av} & -R_{22}^{av} & \delta - R_{23}^{av} & 0 \\ J' - R_{13}^{av} & -\delta - R_{23}^{av} & -R_{33}^{av} & 0 \\ -R_{14}^{av} & 0 & 0 & -R_{44}^{av} \end{pmatrix}\begin{pmatrix} M_1 \\ M_2 \\ M_3 \\ M_4 \end{pmatrix} + \begin{pmatrix} R_{11}^{av} & R_{12}^{av} & R_{13}^{av} & R_{14}^{av} \\ R_{12}^{av} & R_{22}^{av} & R_{23}^{av} & 0 \\ R_{13}^{av} & R_{23}^{av} & R_{33}^{av} & 0 \\ R_{14}^{av} & 0 & 0 & R_{44}^{av} \end{pmatrix}\begin{pmatrix} M_1^{eq} \\ M_2^{eq} \\ M_3^{eq} \\ M_4^{eq} \end{pmatrix}, \quad [8]$$

where $\delta = (\omega_k^e - \omega_l^e)$ and $J' = \pi J\sin(\theta_k)\sin(\theta_l)$. Since the various modes interconvert during the course of the spin lock (as is evident from [7]), the auto- and cross-relaxation rates of the modes are the averages of the relaxation rates of the individual modes weighted by the time spent as each of these modes. These average relaxation rates R_{ij}^{av}, in [8] can be written as (*18*, *19*)

$$R_{ij}^{av} = \frac{1}{\tau}[\mathrm{Tr}(M_i^+ M_i)]^{-1}\int_0^\tau \mathrm{Tr}[M_i(t)^+\Gamma M_j(t)]dt. \quad [9]$$

Thus the average relaxation rates may be calculated using [7] and [9]. These rates are given in Table 1.

It is more convenient to analyze the relaxation rates in terms of those in the regular rotating frame rather than in the spin-locked frame. It should be realized that the relaxation rates when written in a spin-locked frame have an implicit dependence on the position of the spin-lock carrier and on its strength, hence on ϕ and q. This is because the

TABLE 1

a) Average auto-relaxation rates

$$R_{11}^{av} = \left[\cos^4(\phi) + \frac{\sin^4(\phi)}{2} + \frac{\cos^2(\phi)\sin^2(\phi)\sin(2q\tau)}{q\tau} + \frac{\sin^4(\phi)\sin(4q\tau)}{8q\tau}\right]R_{11}$$
$$+ \frac{\sin^2(2\phi)}{32q\tau}[12q\tau - 8\sin(2q\tau) + \sin(4q\tau)]R_{22}$$
$$+ \frac{\sin^2(\phi)}{8q\tau}[4q\tau - \sin(4q\tau)]R_{33}$$

$$R_{22}^{av} = \frac{\sin^2(2\phi)}{32q\tau}[12q\tau - 8\sin(2q\tau) + \sin(4q\tau)]R_{11}$$
$$+ \left[\sin^4(\phi) + \frac{\cos^4(\phi)}{2} + \frac{\sin^2(\phi)\cos^2(\phi)\sin(2q\tau)}{q\tau} + \frac{\cos^4(\phi)\sin(4q\tau)}{8q\tau}\right]R_{22}$$
$$+ \frac{\cos^2(\phi)}{8q\tau}[4q\tau - \sin(4q\tau)]R_{33}$$

$$R_{33}^{av} = \frac{\sin^2(\phi)}{8q\tau}[4q\tau - \sin(4q\tau)]R_{11} + \frac{\cos^2(\phi)}{8q\tau}[4q\tau - \sin(4q\tau)]R_{22}$$
$$+ \left[\frac{1}{2} + \frac{\sin(4q\tau)}{8q\tau}\right]R_{33}$$

$$R_{44}^{av} = R_{44}$$

b) Average cross-relaxation rates

$$R_{12}^{av} = \frac{\sin(2\phi)}{64q\tau}[8q\tau + 24q\tau\cos(2\phi) - 2\sin(4q\tau) - \sin(2\phi - 4q\tau)$$
$$+ 8\sin(2\phi - 2q\tau) - 8\sin(2\phi + 2q\tau) + \sin(2\phi + 4q\tau)]R_{11}$$
$$+ \frac{\sin(2\phi)}{64q\tau}[8q\tau - 24\cos(2\phi) - 2\sin(4q\tau) + \sin(2\phi - 4q\tau)$$
$$- 8\sin(2\phi - 2q\tau) + 8\sin(2\phi + 4q\tau) - \sin(2\phi + 4q\tau)]R_{22}$$
$$+ \frac{\sin(2\phi)}{16q\tau}[\sin(4q\tau) - 4q\tau]R_{33}$$

$$R_{13}^{av} = \frac{1}{q\tau}\left[\frac{5\sin(\phi) + \sin(3\phi)}{16} - \frac{\cos^2(2q\tau)\sin^3(\phi)}{4} - \frac{\cos^2(\phi)\cos(2q\tau)\sin(\phi)}{2}\right]R_{11}$$
$$+ \frac{\sin(2\phi)\cos(\phi)}{8q\tau}[2\cos(2q\tau) - \cos(4q\tau) - 1]R_{22} - \frac{\sin(\phi)\sin^2(2q\tau)}{4q\tau}R_{33}$$

$$R_{23}^{av} = \frac{\cos(\phi)\sin^2(\phi)\sin^4(q\tau)}{q\tau}R_{11}$$
$$+ \frac{1}{q\tau}\left[\frac{\cos(\phi)\cos(2q\tau)\sin^2(\phi)}{2} + \frac{\cos^3(\phi)\cos^2(2q\tau)}{4} + \frac{\cos(3\phi) - 5\cos(\phi)}{16}\right]R_{22}$$
$$+ \frac{\cos(\phi)\sin^2(2q\tau)}{4q\tau}R_{33}$$

$$R_{14}^{av} = \left[\cos^2(\phi) + \frac{\sin^2(\phi)\sin(2q\tau)}{2q\tau}\right]R_{14}$$

projection of the locked frame operators onto the simple rotating frame operators is dependent on the strength and the carrier position of the lock field (see Appendix).

The change in the bandwidth of the HOHAHA onset as the correlation time changes can be understood by the fact that while the sampling of the various modes (the coefficients of the R_{ij} in Table 1) is independent of the correlation time, the relative magnitudes of the R_{ij} are not.

We will interpret the relaxation behavior of the mode M_1 in two specified limits where the magnetization modes and hence their relaxation rates have a simple relationship with the regular rotating frame operators, in order to illustrate this effect. In the limit when both spins are unlocked, i.e., ($\theta_k = \theta_l = 0$ and $\phi = 0$), M_1 is uncoupled from all the other modes, and is represented by $1/2(I_{kz} - I_{lz})$. $R_{11}^{av} = R_{11}$, in this case, is given by

$$R_{11} = d[2J(0) + 3J(\omega)], \qquad [10]$$

where $d = 1/4(\hbar\gamma^2/r^3)^2$. In this limit, $R_{14}^{av} = R_{14}$ which is equal to half the difference between the relaxation rates of I_{kz} and I_{lz}, which are equal. Hence $R_{14} = 0$ and the relaxation of M_1 is monoexponential. Thus, in this limit, which is far from Hartmann–Hahn match the relaxation rate of M_1, which we call $[R_1]^{off} = R_{11}$. This is rate is equivalent to $2dJ(0)$ and $5dJ(0)$ for large and small molecules respectively.

In the limit of perfect Hartmann–Hahn match ($\phi = \pi/2$, $\theta_k = \theta_l \sim \pi/2$), the mode M_1, which may be written in terms of the regular rotating frame operators as $1/2(I_{ky} - I_{ly})$, is periodically converted to M_3, which can be written as $1/2(2I_{kx}I_{lz} - 2I_{kz}I_{lx})$. In this case, the relevant average relaxation rates are given by

$$R_{11}^{av} = \left[\frac{1}{2} + \frac{\sin(2\pi J\tau)}{4\pi J\tau}\right]R_{11} + \left[\frac{1}{2} - \frac{\sin(2\pi J\tau)}{4\pi J\tau}\right]R_{33} \qquad [11a]$$

$$R_{13}^{av} = \frac{\sin^2(\pi J\tau)}{2\pi J\tau}(R_{11} - R_{33}) \qquad [11b]$$

$$R_{14}^{av} = \frac{\sin(\pi J\tau)}{\pi J\tau}R_{14} \qquad [11c]$$

and $R_{23}^{av} = 0$. In this limit, R_{11} and R_{33} are given by

$$R_{11} = R_{33} = \frac{d}{2}[J(0) + 3J(\omega) + 6J(2\omega)]. \qquad [12]$$

Hence, we see from [11b] that $R_{13} = 0$. R_{14}, in this case, is equal to half the difference between the relaxation rates of I_{ky} and I_{ly} which are equal and hence $R_{14} = 0$. Thus the relaxation of the mode M_1 is also monoexponential in this limit. The decay rate $[R_1]^{on} = R_{11}$, which is $dJ(0)/2$ and $5dJ(0)$ for large and small molecules respectively. Thus the ratio $[R_1]^{on}/[R_1]^{off} = 0.25$ for large molecules and 1.0 for small molecules. It is therefore evident that large molecules experience enhanced relaxation far from Hartmann–Hahn match, whereas there is no such enhancement for small molecules.

In the preceding paragraph, we did not consider the effects of transfers orthogonal to the spin-lock axis, in our discussion. These terms do have an effect on the bandwidth of the onset of HOHAHA effects. This is evident from the fact that the introduction of field inhomogeneity effects to which

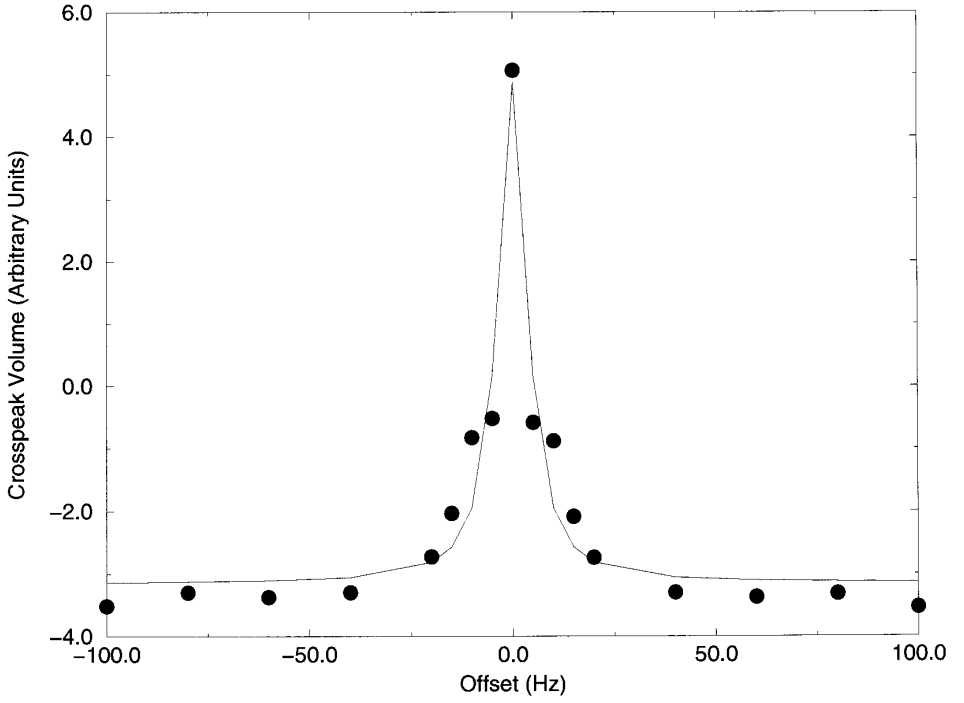

FIG. 6. Plot of the change in the $k \rightarrow l$ crosspeak volume with change in offset for a correlation time of 1.0 ns. Depicted are the calculated crosspeak volumes for various values of the offset and the Lorentzian fitted through the data points.

these terms are susceptible causes a decrease in the bandwidth irrespective of the correlation time, a fact mentioned previously. However, our objective here was to simply provide a simple rationalization for the offset dependence of relaxation effects.

For completeness, and to allow a more direct comparison to experimental observations of Chan *et al.* (*7*), we performed a simulation of the complete 2D experiment depicted in Fig. 1. It is to be remembered that the initial conditions for the transfer are also a little different in this case, since the sampling of I_{ky} or I_{kx} and $-I_{ky}$ or $-I_{kx}$ depends on precession during t_1. Also, no inhomogeneity effects were included in the simulations, since their inclusion increases CPU time by several orders of magnitude. The data were collected using the same spin-system parameters mentioned above, acquiring 512 points in both dimensions. The data were processed using a Kaiser window with a window parameter of 8 and zero-filled to double the size in both dimensions. All data processing was carried out using Felix 95.0 software from Biosym/MSI, San Diego, CA. The $k \rightarrow l$ crosspeak volume was measured as a function of carrier offset. The bandwidth of HOHAHA onset was determined by fitting a Lorentzian through the data (an example is shown in Fig. 6); this is plotted as a function of correlation time in Fig. 7.

The changes with variation in the correlation time, as seen in our simulations, are in qualitative agreement with those reported by Chan *et al.* (*7*); the bandwidth increases with decreasing correlation time. The absolute magnitude of the bandwidths of HOHAHA onset in our simulations are, however, quite different from those obtained experimentally (they are about a factor of 3 less—calculated using rigid isotropic tumbling for the experimental peptides). This could be due to several factors, foremost among them is the fact that in the experimental work (*7*) Chan *et al.* looked at the methyl–methine crosspeak which would be an AX_3 system as opposed to the AX system treated here. Preliminary calculations do show that if the spins considered in our discussion cross-relax with a third spin, the magnitude of the bandwidth is increased. The principles of simulation outlined here could obviously be extended to AX_2 and AX_3 systems.

APPENDIX

The Hamiltonian for two scalar coupled spins k and l in the presence of a spin-lock field of amplitude ω_1, applied along the y axis, is given by

$$H = (\omega_0 - \omega_k)I_{kz} + (\omega_0 - \omega_l)I_{lz} + \omega_1(I_{ky} + I_{ly}) + 2\pi J I_k I_l. \quad [1]$$

To study the behavior of the various density operator components it is more convenient to work in the frame of the spin-lock field. This is achieved by the unitary transformation

$$H_r = U_R H U_R^{-1}$$
$$U_R = e^{-i(\theta_k I_{kx} + \theta_l I_{lx})}, \quad [2]$$

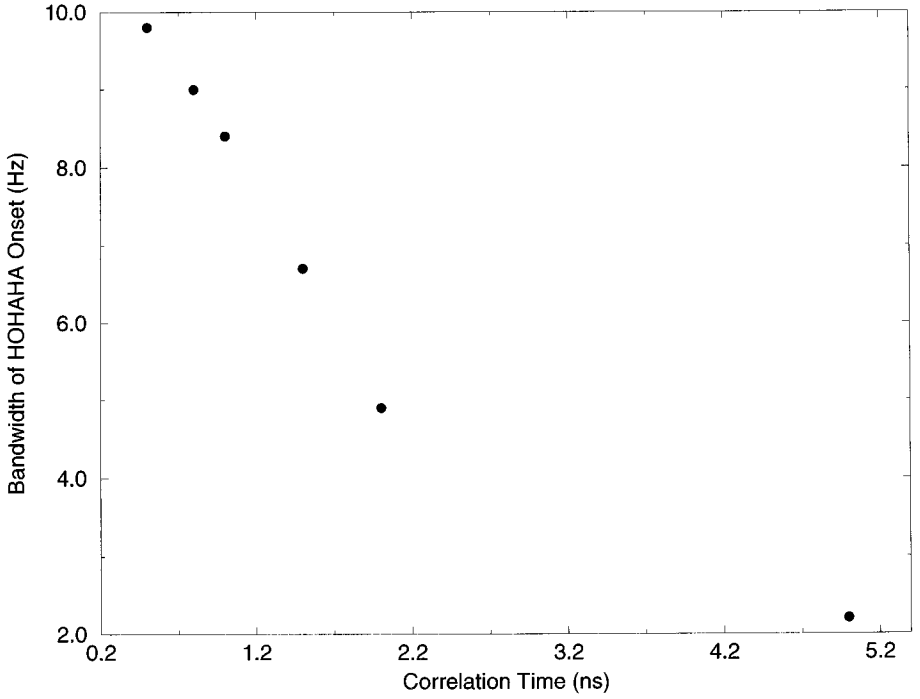

FIG. 7. Plot of the bandwidth of HOHAHA onset against correlation time for the change in the volume of the $k \rightarrow l$ crosspeak with change in the position of the spin-lock transmitter.

where the lock angles and the effective fields are given by $\theta_i = \tan^{-1}[\omega_1/(\omega_0 - \omega_i)]$ and $\omega_i^{e2} = [\omega_1^2 + (\omega_0 - \omega_i)^2]$ respectively, where $i = k, l$. The complete transformed Hamiltonian in the frame of the spin lock (including all nonsecular terms) is given by

$$\begin{aligned} H_R = {} & \omega_k^e I_{kz'} + \omega_l^e I_{lz'} + 2\pi J I_{kz'} I_{lz'} \cos(\theta_k - \theta_l) \\ & + \frac{\pi J[1 + \cos(\theta_k - \theta_l)]}{2} [I_{k+'} I_{l-'} + I_{k-'} I_{l+'}] \\ & + \pi J \sin(\theta_l - \theta_k)[I_{k+'} I_{lz'} + I_{k-'} I_{lz'}] \\ & + \pi J \sin(\theta_k - \theta_l)[I_{kz'} I_{l+'} + I_{kz'} I_{l-'}] \\ & + \frac{\pi J[\cos(\theta_k - \theta_l) - 1]}{2} [I_{k+'} I_{l+'} + I_{k-'} I_{l-'}]. \quad [3] \end{aligned}$$

The spin-operators in the frame of the spin lock are represented by $I_{i\delta'}$ where $i = k, l$ and $\delta = +, -, z$. These may be written in terms of the regular rotating-frame operators as

$$\begin{aligned} I_{iz'} &= I_{iz}\cos(\theta_i) + I_{iy}\sin(\theta_i) \\ I_{iy'} &= I_{iy}\cos(\theta_i) - I_{iz}\sin(\theta_i) \\ I_{ix'} &= I_{ix} \\ I_{i\pm'} &= I_{ix'} \pm iI_{iy'}. \end{aligned} \quad [4]$$

The single- and double-quantum terms in [3] oscillate too rapidly to perturb the eigenstates of the system and may be neglected. Thus [3] transforms to

$$\begin{aligned} H_R = {} & \omega_k^e I_{kz'} + \omega_l^e I_{lz'} + 2\pi J I_{kz'} I_{lz'} \cos(\theta_k - \theta_l) \\ & + \frac{\pi J[1 + \cos(\theta_k - \theta_l)]}{2} [I_{k+'} I_{l-'} + I_{k-'} I_{l+'}]. \quad [5] \end{aligned}$$

For weakly coupled spin systems, [5] may be further simplified to yield

$$\begin{aligned} H_R = {} & \omega_k^e I_{kz'} + \omega_l^e I_{lz'} + 2\pi J \cos(\theta_k)\cos(\theta_l) I_{kz'} I_{lz'} \\ & + \frac{\pi J \sin(\theta_k)\sin(\theta_l)}{2} [I_{k'}^+ I_{l'}^- + I_{k'}^- I_{l'}^+]. \end{aligned} \quad [6]$$

For the very first t_1 point the relevant part of the density matrix is given by I_{ky} which transforms as $I_{ky'}\cos(\theta_k) - I_{kz'}\sin(\theta_k)$. As is evident, $I_{kz'}$ lies along the axis of the spin lock, whereas $I_{ky'}$ is orthogonal to it and hence precesses about the effective field with frequency ω_k^e. For other t_1 points, ignoring relaxation effects, evolution of I_{ky} during t_1 creates terms such as I_{kx}, $2I_{ky}I_{lz}$, and $2I_{kx}I_{lz}$. Taking these terms one by one we see I_{kx} transforms as $I_{kx'}$ which precesses about the effective field with frequency ω_k^e. The be-

havior of the two antiphase terms under the influence of the spin-lock field is given by

$$2I_{kx}I_{lz} \rightarrow \frac{i}{2}[(I_{k+'}I_{l+'} - I_{k-'}I_{l-'}) - (I_{k+'}I_{l-'} - I_{k-'}I_{l+'})]\sin(\theta_l) + [I_{k+'}I_{lz'} + I_{k-'}I_{lz'}]\cos(\theta_l) \quad [7a]$$

$$2I_{ky}I_{lz} \rightarrow \frac{1}{2}[(I_{k+'}I_{l+'} + I_{k-'}I_{l-'}) - (I_{k+'}I_{l-'} + I_{k-'}I_{l+'})]\cos(\theta_k)\sin(\theta_l) - i[I_{k+'}I_{lz'} - I_{k-'}I_{lz'}]\cos(\theta_k)\cos(\theta_l) + i[I_{kz'}I_{l+'} - I_{kz'}I_{l-'}]\sin(\theta_k)\sin(\theta_l) + 2I_{kz'}I_{lz'}\sin(\theta_k)\cos(\theta_l). \quad [7b]$$

Thus, it is evident from [7a], [7b] that under relatively strong spin-lock fields, i.e., $\cos(\theta_k)$, $\cos(\theta_l) \sim 0$, the bulk of $2I_{ky}I_{lz}$ transforms as antiphase and precesses about the effective field with frequency ω_k^e or ω_l^e. On the other hand most of the $2I_{kx}I_{lz}$ component transforms as a mixture of zero- and double-quantum terms which precess with frequencies $(\omega_k^e - \omega_l^e)$ and $(\omega_l^e + \omega_l^e)$ respectively. The precession frequency of the former term is quite small in the case of homonuclear systems under these conditions.

ACKNOWLEDGMENTS

We thank J. R. Tolman and Dr. Scott A. Smith for helpful discussions. This work was supported by Grant GM 33225 from the National Institutes of Health.

REFERENCES

1. A. A. Bothner-By, R. L. Stephens, J. Lee, C. Warren, and R. W. Jeanloz, Structure determination of a tetrasaccharide: Transient Overhauser effects in the rotating frame, *J. Am. Chem. Soc.* **106,** 811–812 (1984).
2. A. Bax and D. G. Davis, Practical aspects of two-dimensional transverse NOE spectroscopy, *J. Magn. Reson.* **63,** 207–213 (1985).
3. C. Griesinger and R. R. Ernst, Frequency offset effects and their elimination in NMR rotating-frame cross-relaxation spectroscopy, *J. Magn. Reson.* **75,** 261–271 (1987).
4. T. L. Hwang and A. J. Shaka, Reliable two-dimensional rotating frame cross-relaxation measurements in coupled spin-systems, *J. Magn. Reson. B* **102,** 155 (1993).
5. T. L. Hwang and A. J. Shaka, Cross-relaxation without TOCSY: Transverse rotating-frame Overhauser spectroscopy, *J. Am. Chem. Soc.* **114,** 3157–3158 (1992).
6. J. Schleucher, J. Quant, S. J. Glaser, and C. Griesinger, A theorem relating cross-relaxation and Hartmann-Hahn transfer in multiple-pulse sequences. Optimal suppression of TOCSY transfer in ROESY, *J. Magn. Reson. A* **112,** 144–151 (1995).
7. T. M. Chan, D. C. Dalgarno, J. H. Prestegard, and C. A. Evans, Choosing a spin lock transmitter position which minimizes HOHAHA distortions of ROESY spectra. Observation of a molecular weight dependence of frequency offset, *J. Magn. Reson.* **126,** 183–186 (1997).
8. S. A. Smith, T. O. Levante, B. H. Meier, and R. R. Ernst, Computer simulations in magnetic resonance. An object-oriented programming approach, *J. Magn. Reson. A* **106,** 75–105 (1994).
9. J. Cavanagh, W. J. Fairbrother, A. G. Palmer III, and N. J. Skelton, ''Protein NMR Spectroscopy Principles and Practice,'' Academic Press, San Diego (1996).
10. R. R. Ernst, G. Bodenhausen, and A. Wokaun, ''Principles of Nuclear Magnetic Resonance in One and Two Dimensions,'' Clarendon Press, Oxford (1987).
11. A. G. Redfield, Theory of relaxation processes, *Adv. Magn. Reson.* **1,** 1–32 (1965).
12. S. A. Smith, W. E. Palke, and J. T. Gerig, Theoretical treatment of relaxation in the presence of an RF field, *J. Magn. Reson.* **100,** 18–24 (1992).
13. C. Griesinger, C. Gemperle, O. W. Sørensen, and R. R. Ernst, Symmetry in coherence transfer. Application to two-dimensional NMR, *Molec. Phys.* **62,** 295–332 (1987).
14. M. Ravikumar, R. Shukla, and A. A. Bothner-By, Relaxation and dynamics of coupled spin systems subjected to continuous radio frequency fields, *J. Chem. Phys.* **95,** 3092–3098 (1991).
15. R. Bazzo and J. Boyd, A theoretical analysis of homonuclear cross-polarization coherence transfer in liquids, *J. Magn. Reson.* **75,** 452–466 (1987).
16. K. L. Ebayed and D. Canet, Behaviour of a coupled two-spin-1/2 system in the presence of a spin-locking radio-frequency field. Relaxation and Hartmann-Hahn transfers, *Molec. Phys.* **71,** 979–993 (1990).
17. L. Muller and R. R. Ernst, Coherence transfer in the rotating frame. Application to heteronuclear cross-correlation spectroscopy, *Molec. Phys.* **38,** 963–992 (1979).
18. J. Briand and R. R. Ernst, Sensitivity comparison of two-dimensional correlation spectroscopy in the laboratory frame and in the rotating frame, *J. Magn. Reson. A* **104,** 54–62 (1993).
19. C. Griesinger and R. R. Ernst, Cross relaxation in time-dependent nuclear spin systems: Invariant trajectory approach, *Chem. Phys. Lett.* **152,** 239–247 (1988).